

---

# Neural Networks Fail to Learn Periodic Functions and How to Fix It

---

Liu Ziyin<sup>1</sup>, Tilman Hartwig<sup>1,2,3</sup>, Masahito Ueda<sup>1,2,4</sup>

<sup>1</sup>Department of Physics, School of Science, The University of Tokyo

<sup>2</sup>Institute for Physics of Intelligence, School of Science, The University of Tokyo

<sup>3</sup>Kavli IPMU (WPI), UTIAS, The University of Tokyo

<sup>4</sup>RIKEN CEMS

## Abstract

Previous literature offers limited clues on how to learn a periodic function using modern neural networks. We start with a study of the extrapolation properties of neural networks; we prove and demonstrate experimentally that the standard activations functions, such as ReLU, tanh, sigmoid, along with their variants, all fail to learn to extrapolate simple periodic functions. We hypothesize that this is due to their lack of a “periodic” inductive bias. As a fix of this problem, we propose a new activation, namely,  $x + \sin^2(x)$ , which achieves the desired periodic inductive bias to learn a periodic function while maintaining a favorable optimization property of the ReLU-based activations. Experimentally, we apply the proposed method to temperature and financial data prediction.

## 1 Introduction

In general, periodic functions are one of the most basic functions of importance to human society and natural science: the world’s daily and yearly cycles are dictated by periodic motions in the Solar System [26]; the human body has an intrinsic biological clock that is periodic in nature [20, 35], the number of passengers on the metro follows daily and weekly modulations, and the stock market experiences (semi-)periodic fluctuations [28, 43]. Global economy also follows complicated and superimposed cycles of different periods, including but not limited to the Kitchin and Juglar cycle [10, 22]. In many scientific scenarios, we want to model a periodic system in order to be able to predict the future evolution, based on current and past observations. While deep neural networks are excellent tools in interpolating between existing data, their fiducial version is not suited to extrapolate beyond the training range, especially not for periodic functions.

If we know beforehand that the problem is periodic, we can easily solve it, e.g., in Fourier space, or after an appropriate transformation. However, in many situations we do not know a priori if the problem is periodic or contains a periodic component. In such cases it is important to have a model that is flexible enough to model both periodic and non-periodic functions, in order to overcome the bias of choosing a certain modelling approach. In fact, despite the importance of being able to model periodic functions, no satisfactory neural network-based method seems to solve this problem. Some previous methods that propose to use periodic activation functions exist [38, 45, 30]. This line of works propose using standard periodic functions such as  $\sin(x)$  and  $\cos(x)$  or their linear combinations as activation functions. However, such activation functions are very hard to optimize due to large degeneracy in local minima [30], and the experimental results suggest that using  $\sin$  as the activation function does not work well except for some very simple model, and that it can not compete against ReLU-based activation functions [34, 7, 25, 42] on standard tasks.

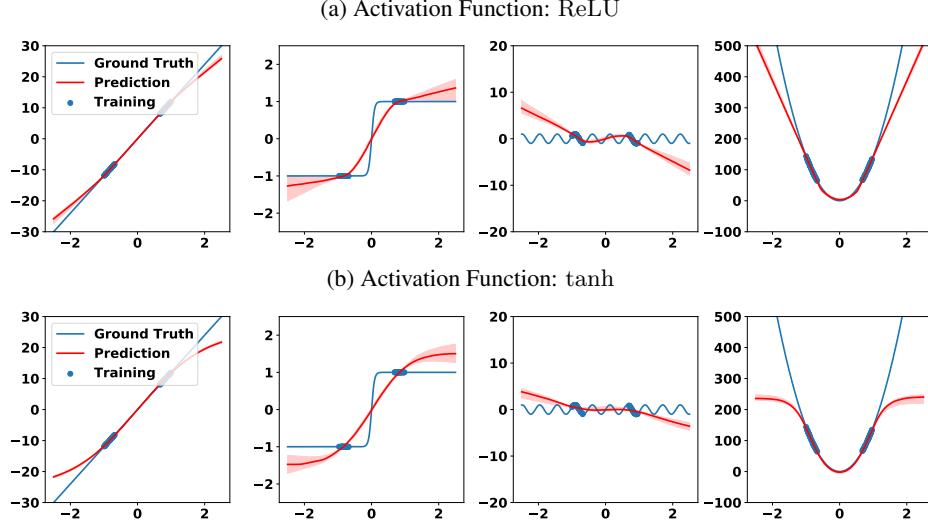


Figure 1: Exploration of how different activation functions extrapolate various basic function types:  $y = x$  (first column),  $y = \tanh(x)$  (second column),  $y = \sin(x)$  (third column), and  $y = x^2$  (last column). The red curves represents the median model prediction and the shaded regions show the 90% credibility interval from 21 independent runs. Note that the horizontal range is re-scaled so that the training data lies between  $-1$  and  $1$ .

The contribution of this work is threefold: (1) we study the extrapolation properties of a neural network beyond a bounded region; (2) we show that standard neural networks with standard activation functions are insufficient to learn periodic functions outside the bounded region where data points are present; (3) we propose a handy solution for this problem and it is shown to work well on toy examples and real tasks. However, the question remains open as to whether better activation functions or methods can be designed.

## 2 Inductive Bias and Extrapolation Properties of Activation Functions

A key property of periodic functions that differentiates them from regular functions is the extrapolation property of such functions. With a period  $2\pi$ , a periodic function  $f(x) = f(x + 2\pi)$  repeats itself *ad infinitum*. Learning a periodic function, therefore, not only requires fitting of pattern on a bounded region, but the learned pattern needs to extrapolate beyond the bounded region. In this section, we experiment with the inductive bias that the common activation functions offer. While it is hard to investigate the effect of using different activation functions in a general setting, one can still hypothesize that the properties of the activation functions are carried over to the property of the neural networks. For example, a tanh network will be smooth and extrapolates to a constant function, while ReLU is piecewise-linear and extrapolates in a linear way.

### 2.1 Extrapolation Experiments

We set up a small experiment in the following way: we use a fully connected neural network with one hidden layer consisting of 512 neurons. We generate training data by sampling from four different analytical functions in the interval  $[-5, 5]$  with a gap in the range  $[-1, 1]$ . This allows us to study the inter-and-extrapolation behaviour of various activation functions. The results can be seen in Fig. 1. This experimental observation, in fact, can be proved theoretically in a more general form. We see that their extrapolation behaviour is dictated by the analytical form of the activation function: ReLU diverges to  $\pm\infty$ , and tanh levels off towards a constant value.

### 2.2 Theoretical Analysis

In this section, we study and prove the *incapability of standard activation functions to extrapolate*.

**Definition 1.** (Feedforward Neural Network.) Let  $f_\sigma(x) = W_h \sigma \dots \sigma W_1 x$  be a function from  $\mathbb{R}^{d_1} \rightarrow \mathbb{R}^{d_{h+1}}$ , where  $\sigma$  is the *activation function* applied element-wise to its input vector, and  $W_i \in \mathbb{R}^{d_i \times d_{i+1}}$ .  $f_\sigma(x)$  is called a *feedforward neural network* with activation function  $\sigma$ , and  $d_1$  is called the input dimension, and  $d_{h+1}$  is the output dimension.

Now, one can show that for arbitrary feedforward neural networks the following two *extrapolation* theorems hold.

**Theorem 1.** Consider a feed forward network  $f_{\text{ReLU}}(x)$ , with arbitrary but fixed depth  $h$  and widths  $d_1, \dots, d_{h+1}$ . Then

$$\lim_{z \rightarrow \infty} \|f_{\text{ReLU}}(zu) - zW_u u - b_u\|_2 = 0, \quad (1)$$

where  $z$  is a real scalar,  $u$  is any unit vector of dimension  $d_1$ , and  $W_u \in \mathbb{R}^{d_1 \times d_h}$  is a constant matrix only dependent on  $u$ .

The above theorem says that any feedforward neural network with ReLU activation converges to a linear transformation  $W_u$  in the asymptotic limit, and this extrapolated linear transformation only depends on  $u$ , the direction of extrapolation. See Figure 1 for illustration. Next, we prove a similar theorem for tanh activation. Naturally, a tanh network extrapolates like a constant function.

**Theorem 2.** Consider a feed forward network  $f_{\text{tanh}}(x)$ , with arbitrarily fixed depth  $h$  and widths  $d_1, \dots, d_{h+1}$ . Then

$$\lim_{z \rightarrow \infty} \|f_{\text{tanh}}(zu) - v_u\|_2 = 0, \quad (2)$$

where  $z$  is a real scalar,  $u$  is any unit vector of dimension  $d_1$ , and  $v_u \in \mathbb{R}^{d_{h+1}}$  is a constant vector that only depends on  $u$ .

We note that these two theorems can be proved through induction, and we give their proofs in the appendix. The above two theorems show that any neural network with ReLU or the tanh activation function cannot extrapolate a periodic function. Moreover, while the specific statement of the theorem applies to tanh and ReLU, it has quite general applicability. Since the proof is only based on the asymptotic property of activation function when  $x \rightarrow \pm\infty$ , one can prove the same theorem for any continuous activation function that asymptotically converges to a tanh or ReLU; for example, this would include Swish and Leaky-ReLU (and almost all the other ReLU-based variants), which converge to ReLU; one can follow the same proving procedure to prove a similar theorem for each of these activation functions.

### 3 Proposed Method: $x + \sin^2(x)$

As we have seen in the previous section, the choice of the activation functions plays a crucial role in affecting the interpolation and extrapolation properties of neural networks, and such interpolation and extrapolation properties in turn affect the generalization of the network equipped with such activation function.

To easily address the proposed function, we propose to use  $x + \sin^2(x)$  as an activation function, which we call the ‘‘Snake’’ function. One can augment it with a factor  $a$  to control the frequency of the periodic part. Thus propose the Snake activation with frequency  $a$

$$\text{Snake}_a := x + \frac{1}{a} \sin^2(ax) = x - \frac{1}{2a} \cos(2ax) + \frac{1}{2a}, \quad (3)$$

We plot Snake for  $a = 0.2, 1, 5$  in Figure 2. We see that larger  $a$  gives higher frequency.

There are also two conceivable alternative choices for a periodicity-biased activation function. One is the sin function, which has been proposed in [30], along with cos and their linear combinations as proposed in Fourier neural networks [45]. However, the problem of these functions does not lie in its generalization ability, but lies in its optimization. In fact, sin is not a monotonic function, and using sin as the activation function creates infinitely many local minima in the solutions (since shifting the preactivation value by  $2\pi$  gives the same function), making sin hard to optimize. See Figure 3 for a comparison on training a 4-layer fully connected neural network on

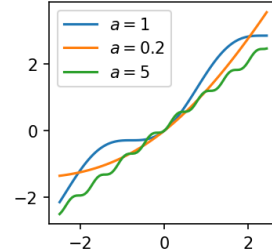


Figure 2: Snake at different  $a$ .

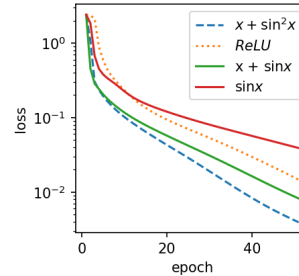


Figure 3: Optimization of different loss functions on MNIST. The proposed activation is shown as a blue dashed curve. We see that Snake is easier to optimize than other periodic baselines. Also interesting is that Snake (and  $x + \sin(x)$ ) are also easier to train than the standard ReLU on this task.

	ReLU	Swish	Tanh	$\sin(x)$	$x + \sin(x)$	$x + \sin^2(x)$
monotonic	✓	✗	✓	✗	✓	✓
(semi-)periodic	✗	✗	✗	✓	✓	✓
first non-linear term	-	$\frac{x^2}{4}$	$-\frac{x^3}{3}$	$-\frac{x^3}{6}$	$-\frac{x^3}{6}$	$x^2$

Table 1: Comparison of different periodic and non-periodic activation functions.

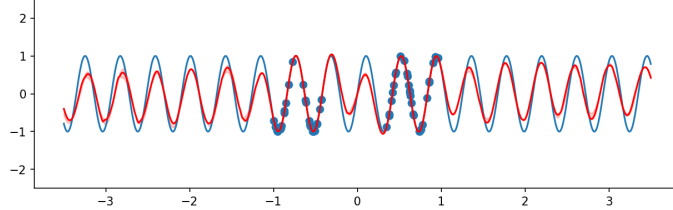


Figure 4: Regressing a simple sin function with Snake as activation functions for  $a = 10$ .

MNIST. We identify the root cause of the problem in sin as its *non-monotonicity*. Since the gradient of model parameters is only a local quantity, it cannot detect the global periodicity of the sin function. Therefore, the difficulty in biasing activation function towards periodicity is that it needs to achieve *monotonicity* and *periodicity* at the same time.

We also propose two other alternatives,  $x + \sin(x)$  and  $x + \cos(x)$ . They are easier to optimize than sin similar to the commonly used ReLU. In the neural architecture search in [34], these two functions are found to be in list of the best-performing activation functions found using reinforcement learning; while they commented that these two are interesting, no further discussion was given regarding their significance. While these two and  $x + \sin^2(x)$  have the same expressive power, we choose  $x + \sin^2(x)$  as the default form of Snake for the following reason. It is important to note that the preactivation values are centered around 0 and the standard initialization schemes such as Kaiming init normalizes such preactivation values to the unit variance [40, 16]. By the law of large numbers, the preactivation roughly obeys a standard normal distribution. This makes 0 a special point for the activation function, since most of preactivation values will lie close to 0. However,  $x + \sin(x)$  seems to be a choice inferior to  $x + \sin^2(x)$  around 0. Expanding around 0:

$$\begin{cases} x + \sin(x) = 2x - \frac{x^3}{6} + \frac{x^5}{120} + o(x^5) \\ x + \sin^2(x) = x + x^2 - \frac{x^4}{3} + o(x^4). \end{cases} \quad (4)$$

Of particular interest to us is the *non-linear term* in the activation, since this is the term that drives the neural network away from its linear counterpart, and learning of a non-linear network is explained by this term to leading order. One finds that the first non-linear order expansion for  $x + \sin(x)$  is already third order, while that of  $x + \sin^2(x)$  is contains a non-vanishing second order term, which can probe non-linear behavior that is odd in  $x$ . We hypothesize that this non-vanishing second order term gives Snake a better approximation property than  $x + \sin(x)$ . In Table 1, we compare the properties of each activation function.

*Extension:* We also suggest the extension to make the  $a$  parameter a learnable parameter for each preactivation value. The benefit for this is that  $a$  no-longer needs to be determined by hand. While we do not study this extension in detail, one experiment is carried out with learnable  $a$ , see the atmospheric temperature prediction experiment in Section 6.2.

### 3.1 Regression with Fully Connected Neural Network

In this section, we regress a simple 1-d periodic function,  $\sin(x)$ , with the proposed activation function. See Figure 4 and compare with the related experiments on tanh and ReLU in Figure 1. As expected, all three activation functions learn to regress the training points. However, neither ReLU nor tanh seems to be able to capture the periodic nature of the underlying function; both baselines inter- and extrapolate in a naive way, with tanh being slightly smoother than ReLU. On the other hand, Snake learns to both interpolate and extrapolate very well, even though the learned amplitude is a little different from the ground truth, it has grasped the correct frequency of the underlying periodic function, both for the interpolation regime and the extrapolation regime. This shows that the proposed method has the desired flexibility towards periodicity, and has the potential to model such problems.

## 4 “Universal Extrapolation Theorem”

In contrast to the well-known universal approximation theorems [19, 8, 12] that qualifies a neural network on a bounded region, we prove a theorem that we refer to as the universal extrapolation theorem, which focuses on the behavior of a neural network with Snake on an unbounded region. This theorem says that a Snake neural network with a sufficient width can approximate any well-behaving periodic function.

**Theorem 3.** *Let  $f(x)$  be a piecewise  $C^1$  periodic function with period  $L$ . Then, a Snake neural network,  $f_{w_N}$ , with one hidden layer and with width  $N$  can converge to  $f(x)$  uniformly as  $N \rightarrow \infty$ , i.e., there exists parameters  $w_N$  for all  $N \in \mathbb{Z}^+$  such that*

$$f(x) = \lim_{N \rightarrow \infty} f_{w_N}(x) \quad (5)$$

for all  $x \in \mathbb{R}$ , i.e., the convergence is point-wise. If  $f(x)$  is continuous, then the convergence is uniform.

As a corollary, this theorem implies the classical approximation theorem [19, 32, 9], which states that a neural network with certain non-linearity can approximate any continuous function on a bounded region.

**Corollary 1.** *Let  $f(x)$  be a two-layer neural network parametrized by two weight matrices  $W_1$  and  $W_2$ , and let  $w$  be the width of the network, then for any bounded and continuous function  $g(x)$  on  $[a, b]$ , there exists  $m$  such that for any  $w \geq m$ , we can find  $W_1, W_2$  such that  $f(x)$  is  $\epsilon$ -close to  $g(x)$ .*

This shows that the proposed activation function is a more general method than the ones previously studied because it has both (1) approximation ability on a bounded region and (2) the ability to learn periodicity on an unbounded region. The practical usefulness of our method is demonstrated experimentally to be on par with standard tasks, and to outperform previous methods significantly on learning periodic functions. Notice that the above theorem not only applies to Snake but also to the basic periodic functions such as  $\sin$  and  $\cos$  and monotonic variants such as  $x + \sin(x)$ ,  $x + \cos(x)$  etc.. While we argued for a preference towards  $x + \sin^2(x)$ , it remains to be determined by large-scale experiments in the industry to decide which one amongst these variants work better in practice, and we do encourage the practitioners to experiment with a few variants to decide the best suitable form for their application.

## 5 Initialization for Snake

As shown in [16], different activation functions actually require different initialization schemes (in terms of the sampling variance) to make the output of each layer unit variance, thus avoiding divergence or vanishing of the forward signal. Let  $W \in \mathbb{R}^{d_1 \times d_2}$ , whose input activations are  $h \in \mathbb{R}^{d_2}$  with a unit variance for each of its element, and the goal is to set the variance of each element in  $W$  such that  $\text{Snake}(Wx)$  has a unit variance. To leading order, Snake looks like an identity function, and so one can make this approximation in finding the required variance:  $\mathbb{E} \left( \sum_j^{d_2} W_{ij} x_j \right)^2 = 1$  which gives  $\mathbb{E}[W_{ij}^2] = 1/\sqrt{d}$ . If we use uniform distribution to initialize  $W$ , then we should sample from  $Uniform(-\sqrt{\frac{3}{d}}, \sqrt{\frac{3}{d}})$ , which is a factor of  $\sqrt{2}$  smaller in range than the Kaiming uniform initialization. We notice that this initialization is often sufficient. However, when higher order correction is necessary, we provide the following exact solution, which is a function of  $a$  in general.

**Proposition 1.** *The variance of expected value of  $x + \frac{\sin^2(ax)}{a}$  under a standard normal distribution is  $\sigma_a^2 = 1 + \frac{1+e^{-8a^2}-2e^{-4a^2}}{8a^2}$ , which is maximized at  $a_{max} \approx 0.56045$ .*

The second term can be thought of as the “response” to the non-linear term  $\sin^2(x)$ . Therefore, one should also correct an additional bias induced by the  $\sin^2(x)$  term by dividing the post-activation value by  $\sigma_a$ . Since the positive effect of this correction is the most pronounced when the network is deep, we compare the difference between having such a correction and having no correction on ResNet-101 on CIFAR-10. The results are presented in the appendix Section A.6.1. We note that using the correction leads to better training speed and better converged accuracy. We find that for standard tasks such as image classification, setting  $0.2 \leq a \leq a_{max}$  to work very well. We thus set the default value of  $a$  to be 0.5. However, for tasks with expected periodicity, larger  $a$ , usually from 5 to 50 tend to work well.

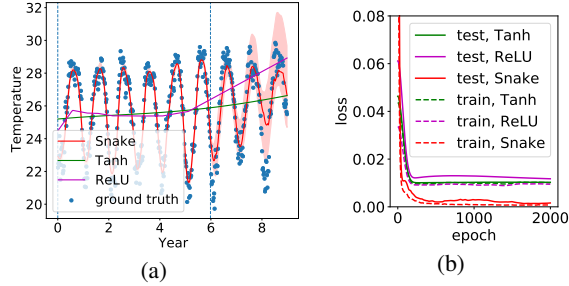


Figure 6: Experiment on the atmospheric data. (a) Regressing the mean weekly temperature evolution of Minamitorishima with different activation functions. For Snake,  $a$  is treated as a learnable parameter and the red contour shows the 90% credibility interval. (b) Comparison of tanh, ReLU, and Snake on a regression task with learnable  $a$ .

## 6 Applications

In this section, we demonstrate the wide applicability of Snake. We start with a standard image classification task, where Snake is shown to perform competitively against the popular activation functions, showing that Snake can be used as a general activation function. We then focus on the tasks where we expect Snake to be very useful, including temperature and financial data prediction. Training in all experiments are stopped at the time when the training loss of all the methods stop to decrease and becomes a constant. The performances of the converged model is not visibly different from the early stopping point for the tasks we considered, and the result would have been similar if we had chosen the early stopping point for comparison<sup>1</sup>.

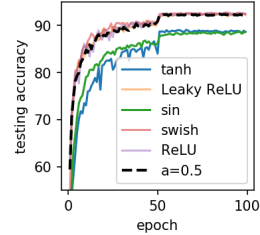


Figure 5: Comparison with other activation functions on CIFAR10.

### 6.1 Image Classification

*Experiment Description.* We train ResNet-18 [17], with roughly 10M parameters, on the standard CIFAR-10 dataset. We simply replace the activation functions in ReLU with the specified ones for comparison. CIFAR-10 is a 10-class image classification task of  $32 \times 32$  pixel images; it is a standard dataset for measuring progress in modern computer vision methods<sup>2</sup>. We use LaProp [46] with the given default hyperparameters as the optimizer. We set learning rates to be  $4e-4$  for the first 50 epochs, and  $4e-5$  for the last 50 epochs. The standard data augmentation technique such as random crop and flip are applied. We note that our implementation reproduces the standard performance of ResNet18 on CIFAR-10, around 92 – 93% testing accuracy. This experiment is designed to test whether Snake is suitable for standard and large-scale tasks one encounters in machine learning. We also compare this result against other standard or recently proposed activation functions including tanh, ReLU, Leaky-ReLU [42], *Swish* [34], and sin [30].

*Result and Discussion.* See Figure 5. We see that sin shows similar performance to tanh, agreeing with what was found in [30], while Snake shows comparative performance to ReLU and Leaky-ReLU both in learning speed and final performance. This hints at the generality of the proposed method, and may be used as a replacement for ReLU in a straightforward way. We also test against other baselines on ResNet-101, which has 4 times more parameters than ResNet-18, to check if Snake can scale up to even larger and deeper networks, and we find that, consistently, Snake achieves similar performance (94.1% accuracy) to the most competitive baselines.

### 6.2 Atmospheric and Body Temperature Prediction

For illustration, we first show two real-life applications of our method to predicting the atmospheric temperature of a local island, and human body temperature. These can be very important for medical applications. Many diseases and epidemics are known to have strong correlation with atmospheric temperature, such as SARS [6] and the current COVID-19 crisis ongoing in the world [44, 36, 27]. Therefore, being able to model temperature accurately could be important for related policy making.

<sup>1</sup>The code for our implementation of a demonstrative experiment can be found at [https://github.com/AdenosHermes/NeurIPS\\_2020\\_Snake](https://github.com/AdenosHermes/NeurIPS_2020_Snake).

<sup>2</sup>Our code is adapted from <https://github.com/kuangliu/pytorch-cifar>

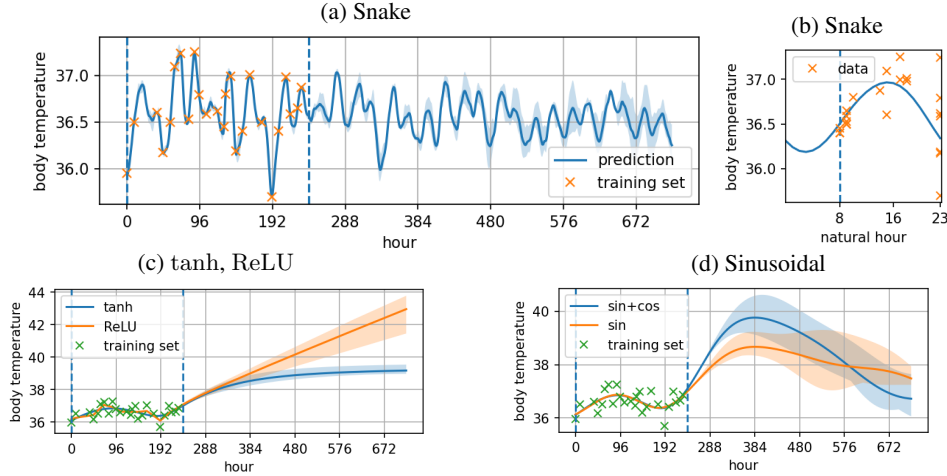


Figure 7: Prediction of human body temperature. (a) Snake; (b) Averaged temperature prediction in a circadian cycle (i.e. as a function of the natural hours in a day); (c) tanh and ReLU; (d) sinusoidal activations.

**Atmospheric temperature prediction.** We start with testing a feedforward neural network with two hidden layers (both with 100 neurons) to regress the temperature evolution in Minamitorishima, an island south of Tokyo (longitude: 153.98, latitude: 24.28)<sup>3</sup>. The data represents the average weekly temperature after April 2008 and the results are shown in Fig. 6a. We see the tanh and ReLU-based models fail to optimize this task, and do not make meaningful extrapolation. On the other hand, the Snake-based model succeeds in optimizing the task and makes meaningful extrapolation with correct period. Also see Figure 6b. We see that Snake achieves vanishing training loss and generalization loss, while the baseline methods all fail to optimize to 0 training loss, and the generalization loss is also not satisfactory. We also compare with the more recent activation functions such as the Leaky-ReLU and Swish, and similar results are observed; see appendix.

**Human body temperature.** Modeling the human body temperature may also be important; for example, fever is known as one of the most important symptom signifying a contagious condition, including COVID19 [15, 39]. *Experiment Description.* We use a feedforward neural network with 2 hidden layers, (both with 64 neurons) to regress the human body temperature. The data is measured irregularly from an anonymous participant over a 10-days period in April, 2020, of 25 measurements in total. While this experiment is also rudimentary in nature, it reflects a great deal of obstacles the community faces, such as very limited (only 25 points for training) and insufficient measurement taken over irregular intervals, when applying deep learning to real problems such as medical or physiological prediction [18, 33]. In particular, we have a dataset where data points from certain period in a day is missing, for example, from 12am to 8am, when the participant is physically at rest (See Figure 7b), and for those data points we have, the intervals between two contiguous measurements are irregular with 8 hours being the average interval, yet this is often the case for medical data where exact control over variables is hard to realize. The goal of this task is to predict the body temperature at *every hour*. The model is trained with SGD with learning rate  $1e-2$  for 1000 steps,  $1e-3$  for another 1000 steps, and  $5e-4$  for another 1000 steps.

*Results and Discussion.* The performances of using ReLU, tanh, sin, sin + cos and Snake are shown in Figure 7. We do not have a testing set for this task, since it is quite unlikely that a model will predict correctly for this problem due to large fluctuations in human body temperature, and we compare the results qualitatively. In fact, we have some basic knowledge about body temperature. For example, (1) it should fall within a reasonable range from 35.5 to 37.5 Celsius degree [13], and, in fact, this is the range where all of the training points lie; (2) at a finer scale, the body temperature follows a periodic behavior, with highest in the afternoon (with a peak at around 4pm), and lowest in the midnight (around 4am) [13]. At the bare minimum, a model needs to obey (1), and a reasonably well-trained model should also discover (2). However, tanh or ReLU fail to limit the temperature to the range 35.5 and 37.5 degree. Both baselines extrapolate to above 39 degree at 20 days beyond the training set. In contrast, learning with Snake as the activation function learned to obey the first rule.

<sup>3</sup>Data from <https://join.fz-juelich.de/access>



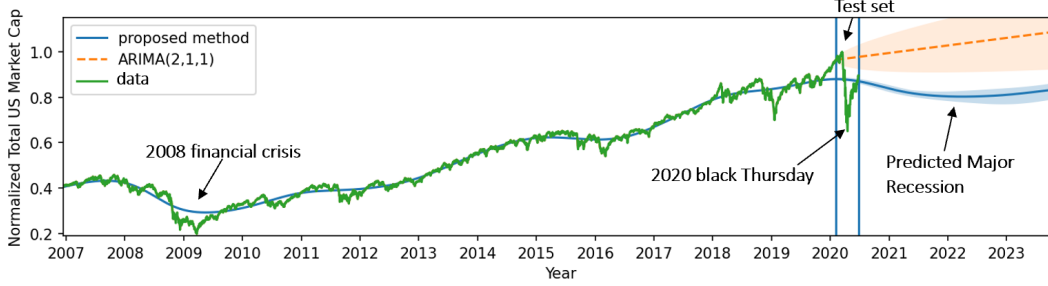


Figure 8: Prediction of Wilshire 5000 index, an indicator of the US and global economy.

See Figure 7.a. To test whether the model has also grasped the periodic behavior specified in (2), we plot the average hourly temperature predicted by the model over a 30 days period. See Figure 7b. We see that the model does capture the periodic oscillation as desired, with peak around 16pm and minimum around 4am. The successful identification of 4am is extremely important, because this is in the range where no data point is present, yet the model inferred correctly the periodic behavior of the problem, showing Snake really captures the correct inductive bias for this problem.

### 6.3 Financial Data Prediction

*Problem Setting.* The global economy is another area where quasi-periodic behaviors might happen [21]. At microscopic level, the economy oscillates in a complex, unpredictable manner; at macroscopic level, the global economy follows a 8 – 10 year cycle that transitions between periods of growth and recession [5, 37]. In this section, we compare different models to predict the total US market capitalization, as measured by the Wilshire 5000 Total Market Full Cap Index<sup>4</sup> (we also did the same experiment on the well-known Buffet indicator, which is seen as strong indicator for predicting national economic trend [24]; we also see similar results). For training, we take the daily data from 1995-1-1 to 2020-1-31, around 6300 points in total, the ending time is deliberately chosen such that it is before the COVID19 starts to affect the global economy [3, 11]. We use the data from 2020 – 2 – 1 to 2020 – 5 – 31 as the test set. Noticeably, the test set differs from training set in two ways (1) a market crash called black Thursday happens (see Figure 8); (2) the general trend is recessive (market cap moving downward on average). It is interesting to see whether the bearish trend in this period is predictable without the affect of COVID19. For neural network based methods, we use a 4-layer feedforward network with  $1 \rightarrow 64 \rightarrow 64 \rightarrow 1$  hidden neurons, with specified activation function, we note that no activation function except Snake could optimize to vanishing training loss. The error is calculated with 5 runs.

*Results and Discussion.* See Table 2, we see that the proposed method outperforms the competitors by a large margin in predicting the market value from 2020-2-1. Qualitatively, we focus on making comparison with ARIMA, a traditional and standard method in economics and stock price prediction [29, 2, 41]. See Figure 8. We note that ARIMA predicts a growing economy, Snake predicts a recessive economy from 2020-2-1 onward. In fact, for all the methods in Table 2, the proposed method is the only method that predicts a recession in and beyond the testing period, we hypothesize that this is because the proposed method is only method that learns to capture the long term economic cycles in the trend. Also, it is interesting that the model predicts a recession without predicting the violent market crash. This might suggest that the market crash is due to the influence of COVID19, while a simultaneous background recession also occurs, potentially due to global business cycle. For purely analysis purpose, we also forecast the prediction until 2023 in Figure 8. Alarmingly, our method predicts a long-term global recession, starting from this May, for an on-average 1.5 year period, only ending around early 2022. This also suggests that COVID19 might not be the only or major cause of the current recessive economy.

Method	MSE on Test Set
ARIMA(2, 1, 1)	0.0215 $\pm$ 0.0075
ARIMA(2, 2, 1)	0.0306 $\pm$ 0.0185
ARIMA(3, 1, 1)	0.0282 $\pm$ 0.0167
ARIMA(2, 1, 2)	0.0267 $\pm$ 0.0154
ReLU DNN	0.0113 $\pm$ 0.0002
Swish DNN	0.0161 $\pm$ 0.0007
sin + cos DNN	0.0661 $\pm$ 0.0936
sin DNN	0.0236 $\pm$ 0.0020
Snake	<b>0.0089<math>\pm</math>0.0002</b>

Table 2: Prediction of Wilshire 5000 Index from 2020-2-1 to 2020-5-31.

<sup>4</sup>Data from <https://www.wilshire.com/indexes>



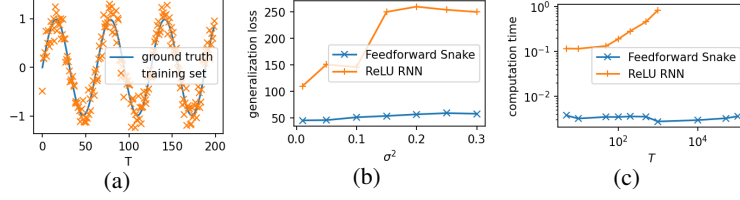


Figure 9: Comparison between simple RNN (with ReLU as activation function) and feedforward network with Snake as activation function. (a) The task is to regress a length- $T$  time series generated by a simple periodic function contaminated with a white gaussian noise with variance  $\sigma^2$ . (b) As the noise increases, the RNN fails in generalization, while this has relatively no effect on the proposed method. (c) One more important advantage of the proposed method is that it requires much less computation time during forward and backward propagation.

#### 6.4 Comparison with RNN on Regressing a Simple Periodic Function

One important application of the learning of periodicities is time series prediction, where the periodicity is at most one-dimensional. This kind of data naturally appears in many audio and textual tasks, such as machine translation [4], audio generation [14], or multimodal learning [23]. Therefore, it is useful to compare with RNN on related tasks. However, we note that the problem with RNNs is that they implicitly parametrize the data point  $x$  by time:  $x = x(t)$ . It is hence limited to model periodic functions of at most 1d and cannot generalize to a periodic function of arbitrary dimension, which is not a problem for our proposed method. We perform a comparison of RNN with Snake deployed on a feedforward network on a 1d problem. See Figure 9.a for the training set of this task. The simple function we try to model is  $y = \sin(0.1x)$ , we add a white noise with variance  $\sigma^2$  to each  $y$ , and the model sees a time series of length  $T$ . See 9.b for the performance of both models, when  $T = 100$ , and validated on a noise-free hold-out section from  $t = 101$  to 300. We see that the proposed method outperforms RNN significantly. On this task, One major advantage of our method is that it does not need to back-propagate through time (BPTT), which both causes vanishing gradient and prohibitively high computation time during training [31]. In Figure 9.c we plot the average computation time of a single gradient update vs. the length of the time series, we see that, even at smallest  $T = 5$ , the RNN requires more than 10 times of computation time to update (when both models have a similar number of parameters, about 3000). For Snake, the training is done with gradient descent on the full batch, and the computation time remains low and does not increase visibly as long as the GPU memory is not overloaded. This is a significant advantage of our method over RNN. Snake can also be used in a recurrent neural network, and is also observed to improve upon ReLU and tanh for predicting long term periodic time evolution. Due to space constraint, we discuss this in section A.2.

## 7 Conclusion

In this work, we have identified the extrapolation properties as a key ingredient for understanding the optimization and generalization of neural networks. Our study of the extrapolation properties of neural networks with standard activation functions suggest the lack of capability to learn a periodic function: due to the mismatched inductive bias, the optimization is hard and generalization beyond the range of observed data points fails. We think that this example suggests that the extrapolation properties of a learned neural networks should deserve much more attention than it currently receives. We then propose a new activation function to solve this periodicity problem, and its effectiveness is demonstrated through the “extrapolation theorem”, and then tested on standard and real-life application experiments. We also hope that our current study will attract more attention to the study of modeling periodic functions using deep learning.

## Acknowledgement

This work was supported by KAKENHI Grant No. JP18H01145, 19K23437, 20K14464, and a Grant-in-Aid for Scientific Research on Innovative Areas “Topological Materials Science” (KAKENHI Grant No. JP15H05855) from the Japan Society for the Promotion of Science. Liu Ziyin thanks the graduate school of science of the University of Tokyo for the financial support he receives. He also thanks Zhang Jie from the depth of his heart; without Zhang Jie’s help, this work could not have

been finished so promptly. We also thank Zhikang Wang and Zongping Gong for offering useful discussions.

## Broader Impact Statement

In the field of deep learning, we hope that this work will attract more attention to the study of how neural networks extrapolate, since how a neural network extrapolates beyond the region it observes data determines how a network generalizes. In terms of applications, this work may have broad practical importance because many processes in nature and in society are periodic in nature. Being able to model periodic functions can have important impact to many fields, including but not limited to physics, economics, biology, and medicine.

## References

- [1] Andreas Antoniou. *Digital signal processing*. McGraw-Hill, 2016.
- [2] Adebisi A Ariyo, Adewumi O Adewumi, and Charles K Ayo. Stock price prediction using the arima model. In *2014 UKSim-AMSS 16th International Conference on Computer Modelling and Simulation*, pages 106–112. IEEE, 2014.
- [3] Andrew Atkeson. What will be the economic impact of covid-19 in the us? rough estimates of disease scenarios. Technical report, National Bureau of Economic Research, 2020.
- [4] Dzmitry Bahdanau, Kyunghyun Cho, and Yoshua Bengio. Neural machine translation by jointly learning to align and translate. *arXiv preprint arXiv:1409.0473*, 2014.
- [5] Fabio Canova. Detrending and business cycle facts. *Journal of monetary economics*, 41(3):475–512, 1998.
- [6] KH Chan, JS Peiris, SY Lam, LLM Poon, KY Yuen, and WH Seto. The effects of temperature and relative humidity on the viability of the sars coronavirus. *Advances in virology*, 2011, 2011.
- [7] Djork-Arné Clevert, Thomas Unterthiner, and Sepp Hochreiter. Fast and accurate deep network learning by exponential linear units (elus). *arXiv preprint arXiv:1511.07289*, 2015.
- [8] Balázs Csanád Csáji et al. Approximation with artificial neural networks. *Faculty of Sciences, Eötvös Loránd University, Hungary*, 24(48):7, 2001.
- [9] George Cybenko. Approximation by superpositions of a sigmoidal function. *Mathematics of control, signals and systems*, 2(4):303–314, 1989.
- [10] Bert De Groot and Philip Hans Franses. Common socio-economic cycle periods. *Technological Forecasting and Social Change*, 79(1):59–68, 2012.
- [11] Nuno Fernandes. Economic effects of coronavirus outbreak (covid-19) on the world economy. Available at SSRN 3557504, 2020.
- [12] Ken-ichi Funahashi and Yuichi Nakamura. Approximation of dynamical systems by continuous time recurrent neural networks. *Neural networks*, 6(6):801–806, 1993.
- [13] Ivayla I Geneva, Brian Cuzzo, Tasaduq Fazili, and Waleed Javaid. Normal body temperature: a systematic review. In *Open Forum Infectious Diseases*, volume 6, page ofz032. Oxford University Press US, 2019.
- [14] Alex Graves. Practical variational inference for neural networks. In *Proceedings of the 24th International Conference on Neural Information Processing Systems, NIPS’ 11*, pages 2348–2356, USA, 2011. Curran Associates Inc.
- [15] Wei-jie Guan, Zheng-yi Ni, Yu Hu, Wen-hua Liang, Chun-quan Ou, Jian-xing He, Lei Liu, Hong Shan, Chun-liang Lei, David SC Hui, et al. Clinical characteristics of coronavirus disease 2019 in china. *New England journal of medicine*, 382(18):1708–1720, 2020.
- [16] Kaiming He, Xiangyu Zhang, Shaoqing Ren, and Jian Sun. Delving deep into rectifiers: Surpassing human-level performance on imagenet classification. In *Proceedings of the IEEE international conference on computer vision*, pages 1026–1034, 2015.

- [17] Kaiming He, Xiangyu Zhang, Shaoqing Ren, and Jian Sun. Deep residual learning for image recognition. In *Proceedings of the IEEE conference on computer vision and pattern recognition*, pages 770–778, 2016.
- [18] Geoffrey Hinton. Deep learning—a technology with the potential to transform health care. *Jama*, 320(11):1101–1102, 2018.
- [19] Kurt Hornik, Maxwell Stinchcombe, Halbert White, et al. Multilayer feedforward networks are universal approximators. *Neural networks*, 2(5):359–366, 1989.
- [20] Norio Ishida, Maki Kaneko, and Ravi Allada. Biological clocks. *Proceedings of the National Academy of Sciences*, 96(16):8819–8820, 1999.
- [21] M Ayhan Kose, Naotaka Sugawara, and Marco E Terrones. Global recessions, 2020.
- [22] Witold Kwasnicki. Kitchin, juglar and kuznetz business cycles revisited. *Wroclaw: Institute of Economic Sciences*, 2008.
- [23] Paul Pu Liang, Ziyin Liu, Amir Zadeh, and Louis-Philippe Morency. Multimodal language analysis with recurrent multistage fusion. *arXiv preprint arXiv:1808.03920*, 2018.
- [24] Jill Mislinski. Market cap to gdp: An updated look at the buffett valuation indicator. *Advisor Perspectives*, 2020.
- [25] Vinod Nair and Geoffrey E Hinton. Rectified linear units improve restricted boltzmann machines. In *Proceedings of the 27th international conference on machine learning (ICML-10)*, pages 807–814, 2010.
- [26] Isaac Newton. *Philosophiae naturalis principia mathematica*. William Dawson & Sons Ltd., London, 1687.
- [27] Alessio Notari. Temperature dependence of covid-19 transmission. *arXiv preprint arXiv:2003.12417*, 2020.
- [28] Denise R. Osborn and Marianne Sensier. The prediction of business cycle phases: Financial variables and international linkages. *National Institute Economic Review*, 182(1):96–105, 2002.
- [29] Ping-Feng Pai and Chih-Sheng Lin. A hybrid arima and support vector machines model in stock price forecasting. *Omega*, 33(6):497–505, 2005.
- [30] Giambattista Parascandolo, Heikki Huttunen, and Tuomas Virtanen. Taming the waves: sine as activation function in deep neural networks, 2016.
- [31] Razvan Pascanu, Tomas Mikolov, and Yoshua Bengio. On the difficulty of training recurrent neural networks. In *International conference on machine learning*, pages 1310–1318, 2013.
- [32] Yang Qu and Ming-Xi Wang. Approximation capabilities of neural networks on unbounded domains. *arXiv preprint arXiv:1910.09293*, 2019.
- [33] Alvin Rajkomar, Jeffrey Dean, and Isaac Kohane. Machine learning in medicine. *New England Journal of Medicine*, 380(14):1347–1358, 2019.
- [34] Prajit Ramachandran, Barret Zoph, and Quoc V Le. Swish: a self-gated activation function. *arXiv preprint arXiv:1710.05941*, 7, 2017.
- [35] Roberto Refinetti and Michael Menaker. The circadian rhythm of body temperature. *Physiology & behavior*, 51(3):613–637, 1992.
- [36] Mohammad M Sajadi, Parham Habibzadeh, Augustin Vintzileos, Shervin Shokouhi, Fernando Miralles-Wilhelm, and Anthony Amoroso. Temperature and latitude analysis to predict potential spread and seasonality for covid-19. *Available at SSRN 3550308*, 2020.
- [37] Matthew D Shapiro and Mark W Watson. Sources of business cycle fluctuations. *NBER Macroeconomics annual*, 3:111–148, 1988.
- [38] Adrian Silvescu. Fourier neural networks. In *IJCNN’99. International Joint Conference on Neural Networks. Proceedings (Cat. No. 99CH36339)*, volume 1, pages 488–491. IEEE, 1999.
- [39] Tanu Singhal. A review of coronavirus disease-2019 (covid-19). *The Indian Journal of Pediatrics*, pages 1–6, 2020.

- [40] Ilya Sutskever, James Martens, George Dahl, and Geoffrey Hinton. On the importance of initialization and momentum in deep learning. In *International conference on machine learning*, pages 1139–1147, 2013.
- [41] Jung-Hua Wang and Jia-Yann Leu. Stock market trend prediction using arima-based neural networks. In *Proceedings of International Conference on Neural Networks (ICNN’96)*, volume 4, pages 2160–2165. IEEE, 1996.
- [42] Bing Xu, Naiyan Wang, Tianqi Chen, and Mu Li. Empirical evaluation of rectified activations in convolutional network. *arXiv preprint arXiv:1505.00853*, 2015.
- [43] Liheng Zhang, Charu Aggarwal, and Guo-Jun Qi. Stock price prediction via discovering multi-frequency trading patterns. In *Proceedings of the 23rd ACM SIGKDD International Conference on Knowledge Discovery and Data Mining, KDD ’17*, page 2141–2149, New York, NY, USA, 2017. Association for Computing Machinery.
- [44] Yongjian Zhu and Jingui Xie. Association between ambient temperature and covid-19 infection in 122 cities from china. *Science of The Total Environment*, page 138201, 2020.
- [45] Abylay Zhumekenov, Malika Uteuliyeva, Olzhas Kabdolov, Rustem Takhanov, Zhenisbek Assylbekov, and Alejandro J. Castro. Fourier neural networks: A comparative study, 2019.
- [46] Liu Ziyin, Zhikang T Wang, and Masahito Ueda. Laprop: a better way to combine momentum with adaptive gradient. *arXiv preprint arXiv:2002.04839*, 2020.

## A Additional Experiments

### A.1 Effect of using different $a$ and More Periodic Function Regressions

It is interesting to study the behavior of the proposed method on different kinds of periodic functions (continuous, discontinuous, compound periodicity). See Figure 10. We see that using different  $a$  seems to bias model towards different frequencies. Larger  $a$  encourages learning with larger frequency and vice versa. For more complicated periodic functions, see Figure 11 and 12.

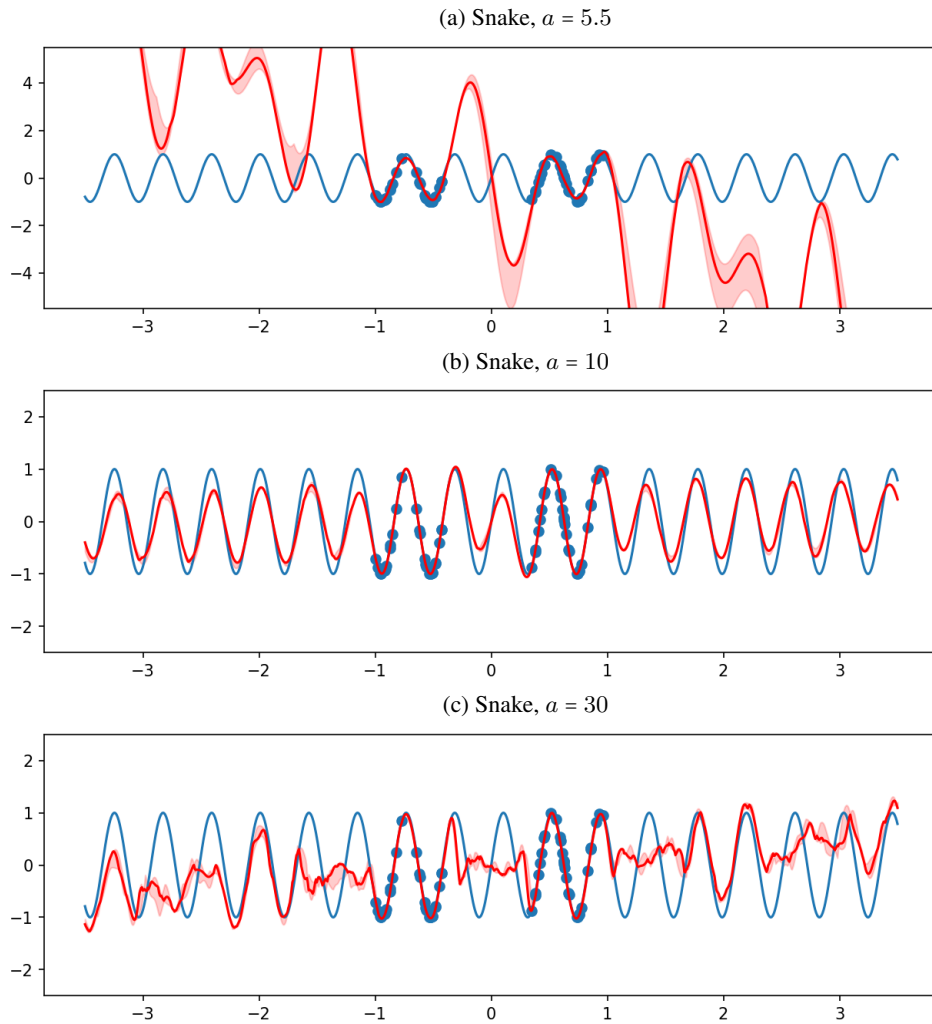
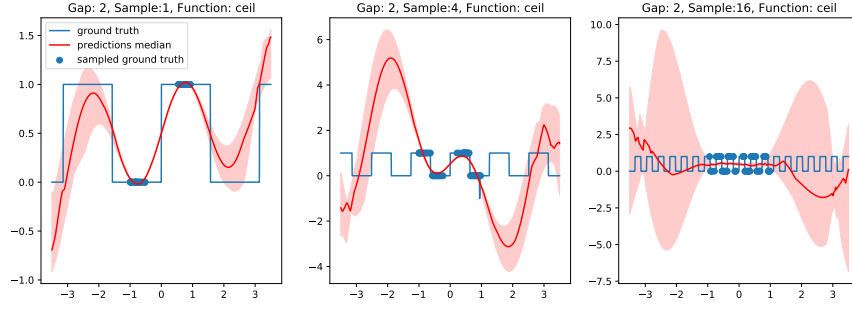


Figure 10: Effect of using different  $a$ .

(a)  $a = 1$



(b)  $a = 16$

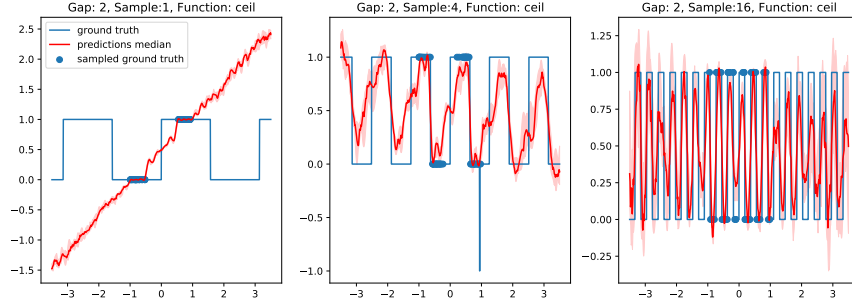
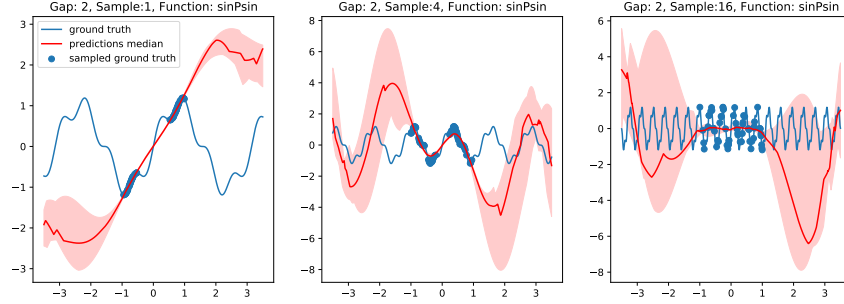


Figure 11: Regressing a rectangular function with Snake as activation function for different values of  $a$ . For a larger value of  $a$ , the extrapolation improves.

(a)  $a = 1$



(b)  $a = 16$

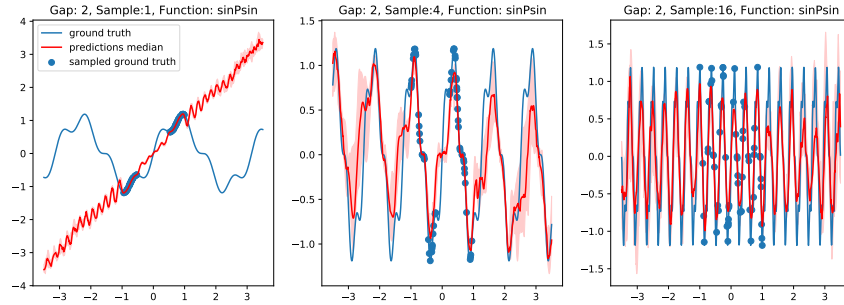


Figure 12: Regressing  $\sin(x) + \sin(4x)/4$  with Snake as activation function for different values of  $a$ . For a larger value of  $a$ , the extrapolation improves: Whereas the  $a = 1$ -model treats the high-frequency modulation as noise, the  $a = 16$ -model seems to learn a second signal with higher frequency (bottom centre).



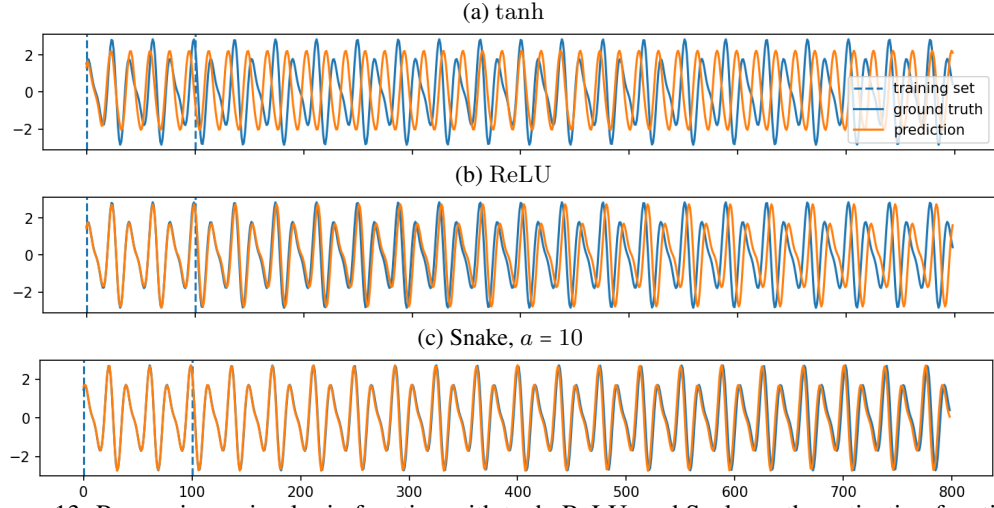


Figure 13: Regressing a simple sin function with tanh, ReLU, and Snake as the activation function.

## A.2 Learning a Periodic Time Evolution

In this section, we try to fit a periodic dynamical system whose evolution is given by  $x(t) = \cos(t/2) + 2\sin(t/3)$ , and we use a simple recurrent neural network as the model, with the standard tanh activation replaced by the designated activation function. We use Adam as the optimizer. See Figure 13. The region within the dashed vertical lines are the range of the training set.

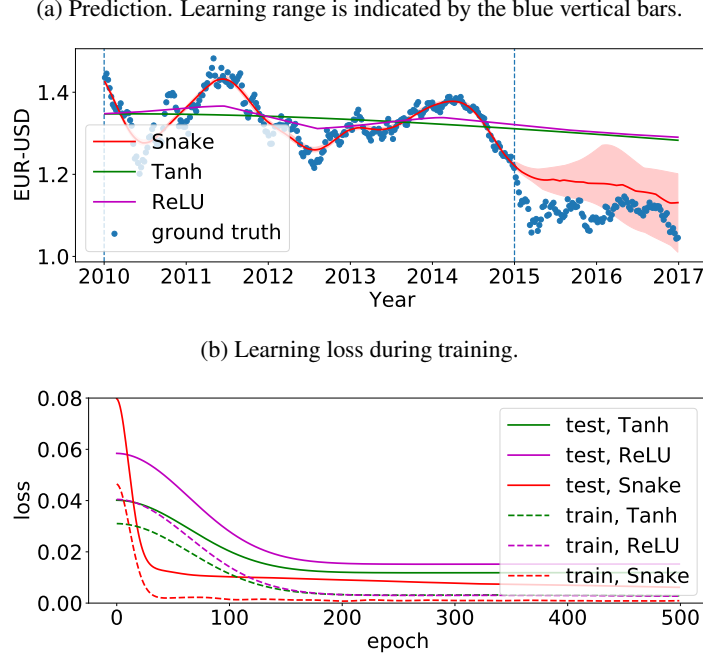


Figure 14: Comparison between Snake, tanh, and ReLU as activation functions to regress and predict the EUR-USD exchange rate.

### A.3 Currency exchange rate modelling

We investigate how Snake performs on one more financial data. The task is to predict the exchange rate between EUR and USD. As in the main text, we use a two-hidden-layer feedforward network with 256 neurons in the first and 64 neurons in the second layer. We train with SGD, with a learning rate of  $10^{-4}$ , weight decay of  $10^{-4}$ , momentum of 0.99, and a mini-batch size of  $16^5$ . For Snake, we make  $a$  a learnable parameter. The result can be seen in Fig. 14. Only Snake can model the rate on the training range and makes the most realistic prediction for the exchange rate beyond the year 2015. The better optimization and generalization property of Snake suggests that it offers the correct inductive bias to model this task.

<sup>5</sup>Hyperparameter exploration performed with Hyperactive: <https://github.com/SimonBlanke/Hyperactive>

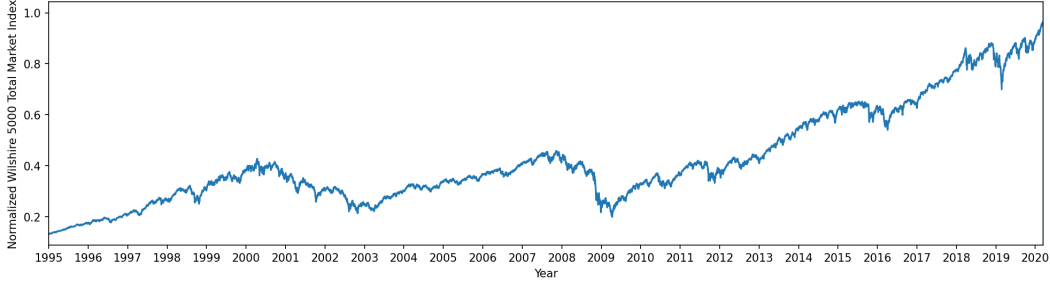


Figure 15: Full Training set for Section 6.3

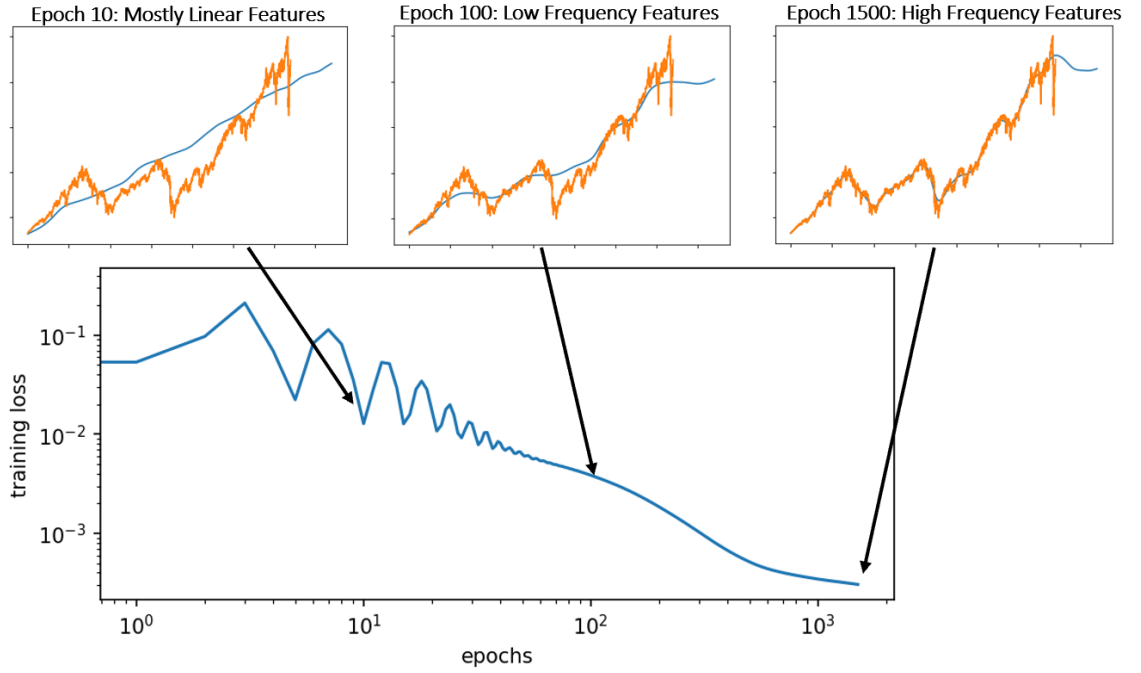


Figure 16: Learning trajectory of Snake. One notices that Snake firsts learns linear features, then low frequency features and then high frequency features.

#### A.4 How does Snake learn?

We take this chance to study the training trajectory of Snake using the market index prediction task as an example. We set  $a = 20$  in this task. See Figure 15 for the full training set for this section (and also for Section 6.3). See Figure 16 for how the learning proceeds. Interestingly, the model first learns an approximately linear function (at epoch 10), and then it learns low frequency features, and then learns the high frequency features. In many problems such as image and signal processing [1], the high frequency features are often associated with noise and are not indicative of the task at hand. This experiment explains in part the good generalization ability that Snake seems to offer. Also, this suggests that one can also devise techniques to early stopping on Snake in order to prevent the learning of high-frequency features when they are considered undesirable to learn.

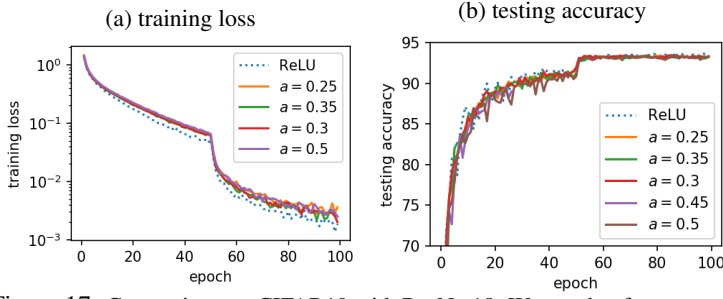


Figure 17: Comparison on CIFAR10 with ResNet18. We see that for a range of choice of  $a$ , there is no discernible difference between the generalization accuracy of ReLU and Snake.

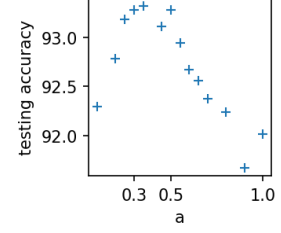


Figure 18: Grid Search for Snake at different  $a$  on ResNet18.

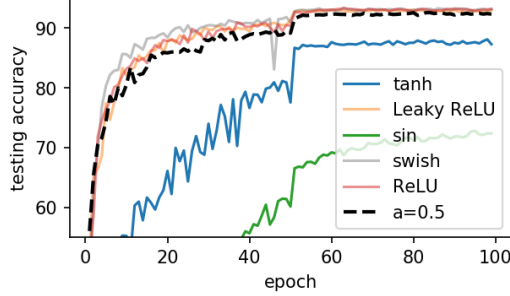


Figure 19: ResNet100 on CIFAR-10. We see that the proposed method achieves comparable performance to the ReLU-style activation functions, significantly better than tanh and sin.

## A.5 CIFAR-10 Figures

In this section, we show that the proposed activation function can achieve performance similar to ReLU, the standard activation function, both in terms of generalization performance and optimization speed. See Figure 17. Both activation functions achieve  $93.5 \pm 1.0\%$  accuracy.

## A.6 CIFAR-10 with ResNet101

To show that Snake can scale up to larger and deep neural networks, we also repeat the experiment on CIFAR-10 with ResNet101. See Figure 19. Again, we see that the Snake achieves similar performance to ReLU and Leaky-ReLU.

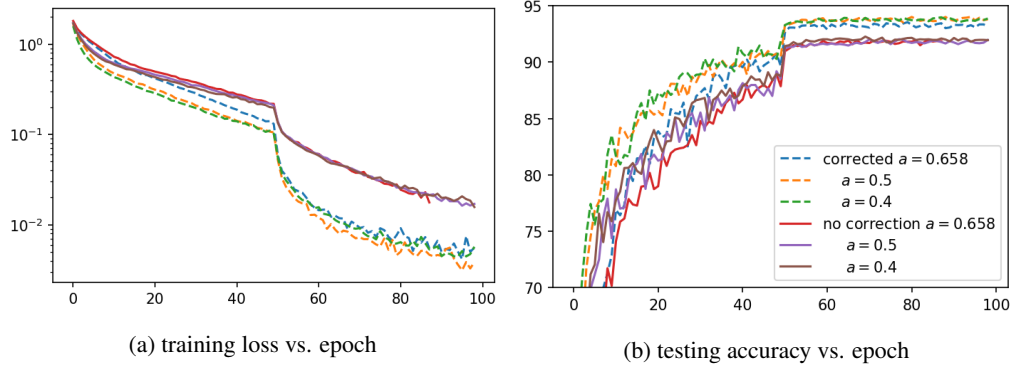


Figure 20: Effect of variance correction

### A.6.1 Effect of Variance Correction

In this section, we show the effect of variance correction is beneficial. Since the positive effect of correction is the most pronounced when the network is deep, we compare the difference between having such correction and having no correction on ResNet101 on CIFAR-10. See Figure 20; we note that using the correction leads to better training speed and better converged accuracy.

We also restate the proposition here.

**Proposition 2.** *The variance of expected value of  $x + \frac{\sin^2(ax)}{a}$  under a standard normal distribution is  $\sigma_a^2 = 1 + \frac{1+e^{-8a^2}-2e^{-4a^2}}{8a^2}$ , which is maximized at  $a_{max} \approx 0.56045$ .*

*Proof.* The proof is straight-forward calculation. The second moment of Snake is  $1 + \frac{3+e^{-8a^2}-4e^{-2a^2}}{8a^2}$ , while the squared first moment is  $\frac{e^{-4a^2}(-1+e^{2a^2})^2}{4a^2}$ , and subtracting the two, we obtain the desired variance

$$\sigma_a^2 = 1 + \frac{1 + e^{-8a^2} - 2e^{-4a^2}}{8a^2}. \quad (6)$$

Solving for this numerically from a numerical solver (we used Mathematica) renders the maximum at  $a_{max} \approx 0.56045$ .  $\square$

## B Proofs for Section 2.2

We reproduce the statements of the theorems for the ease of reference.

**Theorem 4.** Consider a feed forward network  $f_{\text{ReLU}}(x)$ , with arbitrary but fixed depth  $h$  and widths  $d_1, \dots, d_{h+1}$ . Then

$$\lim_{z \rightarrow \infty} \|f_{\text{ReLU}}(zu) - zW_u u - b_u\|_2 = 0, \quad (7)$$

where  $z$  is a real scalar,  $u$  is any unit vector of dimension  $d_1$ , and  $W_u \in \mathbb{R}^{d_1 \times d_h}$  is a constant matrix only dependent on  $u$ .

We prove this by induction on  $h$ . We first prove the base case when  $h = 2$ , i.e., a simple non-linear neural network with one hidden layer.

**Lemma 1.** Consider feed forward network  $f_{\text{ReLU}}(x)$  with  $h = 2$ . Then

$$\lim_{z \rightarrow \infty} \|f_{\text{ReLU}}(zu) - zW_u u - b_u\|_2 = 0 \quad (8)$$

for all unit vector  $u$ .

*Proof.* In this case,

$$f_{\text{ReLU}}(x) = W_2 \sigma(W_1 x + b_1) + b_2,$$

where  $\sigma(x) = \text{ReLU}(x)$ , and let  $\mathbf{1}_{x>0}$  denote the vector that is 1 when  $x > 0$  and zero otherwise, and let  $M_{x>0} := \text{diag}(\mathbf{1}_{x>0})$ , then for any fixed  $u$  we have

$$f_{\text{ReLU}}(zu) = W_2 M_{W_1 zu + b_1 > 0} (W_1 zu + b_1) + b_2 = zW_u u + b_u \quad (9)$$

where  $W_u := W_2 M_{W_1 zu + b_1 > 0} W_1$  and  $b_u = W_u b_1 + b_2$ , and  $W_u$  is the desired linear transformation and  $b_u$  the desired bias; we are done.  $\square$

Apparently, due the self-similar structure of a deep feedforward network, the above argument can be iterated over for every layer, and this motivates for a proof based on induction.

*Proof of Theorem.* Now we induce on  $h$ . Let the theorem hold for any  $h \leq n$ , and we want to show that it also holds for  $h = n + 1$ . Let  $h = n + 1$ , we note that any  $f_{\text{ReLU}, h=n+1}$  can be written as

$$f_{\text{ReLU}, h=n+1}(zu) = f_{\text{ReLU}, h=2}(f_{\text{ReLU}, h=n}(zu)) \quad (10)$$

then, by assumption,  $f_{\text{ReLU}, h=n}(x)$  approaches  $zW_u u + b_u$  for some linear transformation  $W_u$ ,  $b_u$ :

$$\lim_{z \rightarrow \infty} f_{\text{ReLU}, h=n+1}(zu) = f_{\text{ReLU}, h=2}(zW_u u + b_u) \quad (11)$$

and, by the lemma, this again converge to a linear transformation, and we are done.  $\square$

Now we can prove the following theorem, this proof is much simpler and does not require induction.

**Theorem 5.** Consider a feed forward network  $f_{\tanh}(x)$ , with arbitrarily fixed depth  $h$  and widths  $d_1, \dots, d_{h+1}$ , then

$$\lim_{z \rightarrow \infty} \|f_{\text{ReLU}}(zu) - v_u\|_2 = 0, \quad (12)$$

where  $z$  is a real scalar, and  $u$  is any unit vector of dimension  $d_1$ , and  $v_u \in \mathbb{R}^{d_{h+1}}$  is a constant vector only depending on  $u$ .

*Proof.* It suffices to consider a two-layer network. Likewise,  $f_{\tanh}(zu) = (W_2 \sigma(W_1 zu + b_1) + b_2)$ , where  $\sigma(x) = \tanh(x)$ . As  $z \rightarrow \infty$ ,  $W_1 zu + b_1$  approaches either positive or negative infinity, and so  $\sigma(W_1 zu + b_1)$  approaches a constant vector whose elements are either 1 or  $-1$ , which is a constant vector, and  $(W_2 \sigma(W_1 zu + b_1) + b_2)$  also approaches some constant vector  $v_u$ .

Now any layer that are composed after the first hidden layer takes in an asymptotically constant vector  $v_u$  as input, and since the activation function  $\tanh$  is a continuous function,  $f_{\tanh}(x)$  is continuous, and so

$$\lim_{z \rightarrow \infty} f_{\tanh, h=n}(x) = f_{\tanh, h=n-1}(v_u) = v'_u. \quad (13)$$

We are done.  $\square$



## C Universal Extrapolation Theorems

**Theorem 6.** *Let  $f(x)$  be a piecewise  $C^1$  periodic function with period  $L$ . Then, a Snake neural network,  $f_{w_N}$ , with one hidden layer and with width  $N$  can converge to  $f(x)$  uniformly as  $N \rightarrow \infty$ , i.e., there exists parameters  $w_N$  for all  $N \in \mathbb{Z}^+$  such that*

$$f(x) = \lim_{N \rightarrow \infty} f_{w_N}(x) \quad (14)$$

for all  $x \in \mathbb{R}$ , i.e., the convergence is point-wise. If  $f(x)$  is continuous, then the convergence is uniform.

We first show that using  $\cos$  as activation function may approximate any periodic function, and then show that Snake may represent a  $\cos$  function exactly.

**Lemma 2.** *Let  $f(x)$  be defined as in the above theorem and let  $f_{w_N}(x)$  be a feedforward neural network with  $\cos$  as the activation function, then  $f_{w_N}(x)$  can converge to  $f(x)$  point-wise.*

*Proof.* It suffices to show that a neural network with  $\sin$  as activation function can represent a Fourier series to arbitrary order, and then apply the Fourier convergence theorem. By the Fourier convergence theorem, we know that

$$f(x) = \frac{a_0}{2} + \sum_{m=1}^{\infty} \left[ \alpha_m \cos\left(\frac{m\pi x}{L}\right) + \beta_m \sin\left(\frac{m\pi x}{L}\right) \right], \quad (15)$$

for unique Fourier coefficients  $\alpha_m, \beta_m$ , and we recall that our network is defined as

$$f_{w_N}(x) = \sum_{i=1}^D w_{2i} \cos(w_{1i}x + b_{1i}) + b_{2i} \quad (16)$$

then we can represent Eq. 15 order by order. For the  $m$ -th order term in the Fourier series, we let

$$w_{2,2m-1} = \beta_m = \int_{-L}^L f(x) \sin\left(\frac{m\pi x}{L}\right) dx \quad (17)$$

$$w_{1,2m-1} = \frac{m\pi}{L} \quad (18)$$

$$w_{2,2m} = \alpha_m = \int_{-L}^L f(x) \cos\left(\frac{m\pi x}{L}\right) dx \quad (19)$$

$$w_{1,2m} = \frac{m\pi}{L} \quad (20)$$

$$b_{1,2m-1} = -\frac{\pi}{2} \quad (21)$$

$$(22)$$

and let the unspecified biases  $b_i$  be 0: we have achieved an exact parametrization of the Fourier series of  $m$  order with a  $\sin$  neural network with  $2m$  many hidden neurons, and we are done.  $\square$

The above proof is done for a  $\cos(x)$  activation; we are still obliged to show that Snake can approximate a  $\cos(x)$  neuron.

**Lemma 3.** *A finite number of Snake neurons can represent a single  $\cos$  activation neuron.*

*Proof.* Since the frequency factor  $a$  in Snake can be removed by a rescaling of the weight matrices, we set  $a = 2$ , and so  $x + \sin^2(x) = x - \cos(x) + \frac{1}{2}$ . We also reverse the sign in front of  $\cos$ , and remove the bias  $\frac{1}{2}$ , and prove this lemma for  $x + \cos(x)$ . We want to show that for a finite  $D$ , there  $w_1$  and  $w_2$  such that

$$\cos(x) = \sum_{i=1}^D w_{2,i}(w_{1,i}x + b_{1,i}) + b_{2,i} + \sum_{i=1}^D w_{2,i} \cos(w_{1,i}x + b_{1,i}) \quad (23)$$

This is achievable for  $D = 2$ , let  $w_{1,1} = -w_{1,2} = 1$ , and let  $b_{1,i} = b_{2,i} = 0$ , we have:

$$\cos(x) = (w_{2,1} - w_{2,2})x + \sum_{i=1}^D w_{2,i} \cos(x) \quad (24)$$

and set  $w_{2,1} = w_{2,2} = \frac{1}{2}$  achieves the desired result. Combining with the result above, this shows that a Snake neural network with  $4m$  many hidden neurons can represent exactly a Fourier series to  $m$ -th order.  $\square$

**Corollary 2.** *Let  $f(x)$  be a two layer neural network parametrized by two weight matrices  $W_1$  and  $W_2$ , and let  $w$  be the width of the network, then for any bounded and continuous function  $g(x)$  on  $[a, b]$ , there exists  $m$  such that for any  $w \geq m$ , we can find  $W_1, W_2$  such that  $f(x)$  is  $\epsilon$ -close to  $g(x)$ .*

*Proof.* This follows immediately by setting  $[a, b]$  to match the  $[-L, L]$  region in the previous theorem.  $\square$